

TRIPLY DIFFERENTIAL PHOTOELECTRON STUDIES OF THE FOUR OUTERMOST VALENCE ORBITALS OF CYANOGEN

D.M.P. HOLLAND

Institute of Physical Science and Technology, University of Maryland, College Park, MD 20742 (U.S.A.)

A.C. PARR and D.L. EDERER

Synchrotron Ultraviolet Radiation Facility, National Bureau of Standards, Washington, DC 20234 (U.S.A.)

J.B. WEST

Daresbury Laboratory, Daresbury, Warrington, WA4 4AD (Gt. Britain)

J.L. DEHMER

Argonne National Laboratory, Argonne, IL 60439 (U.S.A.)

(First received 14 December 1982; in final form 1 March 1983)

ABSTRACT

Photoelectron measurements, differential in incident wavelength, photoelectron energy and photoelectron ejection angle, have been performed on cyanogen, C_2N_2 , from threshold to a photon energy of 24 eV, using synchrotron radiation. The results are presented in the form of photoionization branching ratios and photoelectron angular distributions, including vibrationally resolved results for the outermost orbital, $1\pi_g$. Some evidence for resonant processes is observed and discussed within the framework of recent work on related molecules. However, reliable assignments require further theoretical guidance with regard to the location and identities of possible shape resonances and autoionizing intravalence transitions in the C_2N_2 spectrum.

INTRODUCTION

Resonant processes, such as shape or autoionizing resonances, play a central role in the study of photoionization dynamics of atoms and molecules [1]. They are usually displayed prominently against non-resonant behavior in such observables as the total photoionization cross-section, photoionization branching ratios and photoelectron angular distributions.

More importantly, the study of resonant features has repeatedly led to a greater physical insight into the mechanisms of excitation, resonant trapping of the photoelectron, and decay of the excited complex, that occur during the photoionization process. These processes can be studied by a variety of techniques [1,2]. However, the combination of synchrotron radiation and angle-resolved photoelectron spectroscopy has been especially fruitful in that the partial cross-sections or branching ratios, and the photoelectron angular distribution parameter β , may be measured directly as a continuous function of wavelength. The characteristic variations of these parameters in the vicinity of a resonance are among the most powerful ways of accessing dynamical information.

A useful conceptual starting point in considering molecular photoionization dynamics is the joint use of the Born–Oppenheimer approximation and the Franck–Condon separation (see, for example, Herzberg [3]). The consequences of this hierarchy of separation of electronic and nuclear motion is, in part, that the relative vibrational intensities within an electronic band will be proportional to their respective Franck–Condon factors. Furthermore, for a given electronic transition, the photoelectron angular distributions will be independent of the vibrational quantum number, v . Although this framework can be expected to be applicable throughout large portions of the spectrum, i.e., for direct photoionization, a variety of circumstances which would cause this view to breakdown at either the Born–Oppenheimer or the Franck–Condon level of approximation may be identified. Examples include shape resonances, autoionization, near-threshold ionization, Cooper zeros, and breakdown of the single-particle model for certain inner valence excitations (see ref. 1 and references cited therein).

The effects of shape resonance and autoionization phenomena have been studied as a continuous function of photon energy in a number of molecules; N_2 [4–8], CO [4,5,9,10], O_2 [1,11–14], NO [15], CO_2 [16], COS [17,18], CS_2 [17,18], C_2H_2 [19–23], and C_2H_4 [24]. However, only a few of the experiments have been performed with sufficient resolution to permit vibrational analysis. Corresponding theoretical work has been done on N_2 [25–32], CO [25,27,29,33–35], O_2 [36–38], NO [39], CO_2 [29,40–43], COS [29], CS_2 [29], C_2H_2 [19,20,44] and C_2H_4 [24]. Much of the early work focused on the first row diatomics, N_2 , CO and O_2 , and it is only recently that such studies have been broadened to include the investigation of vibrational effects in polyatomic molecules. In particular, a vibrationally resolved photoionization study [21] of C_2H_2 , which is isoelectronic with N_2 and CO proved very instructive. The interpretation contained significant departures from that which would have been suggested by a naive extrapolation of the results for N_2 and CO . In so doing, this study made it obvious that our scope should be extended systematically to other molecules in order to broaden and deepen

an understanding of dynamical effects in the photoionization of small molecules.

In this paper, triply differential photoelectron studies on cyanogen, C_2N_2 , are reported from close to the first ionization threshold to a photon energy of 24 eV. This choice was motivated by the fact that cyanogen is a larger molecule than those indicated above, but, nevertheless, contains a $C\equiv N$ bond which is closely related to the bonds in the extensively studied first row diatomic molecules. Moreover, a possibility of shape resonant trapping exists not only on the $C\equiv N$ component, but also on the $C-C$ bond. Also, the off-center location of the CN group may result in positive and negative linear combinations of trapping sites. These trapping sites in the context of shape resonances are the result of centrifugal and electrostatic forces combining to give a net positive potential for some ranges of electron coordinates (see, for example, refs. 1 and 45). The effects of placing the CN group in various chemical environments, e.g., C_2N_2 , HCN, and CH_3CN , has been investigated, but the latter two will be discussed elsewhere [46,47]. In the present work, we are unfortunately beyond present theoretical progress, as no calculations have been performed on the role of autoionization or shape resonances in the dynamics of C_2N_2 photoionization. Therefore, the experimental results are reported together with a necessarily limited discussion in order to stimulate theoretical investigations of this interesting case. Indeed, non-Franck-Condon behavior is observed for the first band $(1\pi_g)^{-1}X^2\Pi_g$, which however requires some theoretical guidance in order to specify the underlying mechanisms. It was not possible to resolve directly the higher vibrational members of the second electronic state because, within the present experimental resolution, these levels coincide with the dominant $v = 0 \rightarrow 0$ transition of the third band. However, deconvolution allowed the asymmetry parameters to be deduced for the $v = 0$ vibrational level in both the A and the B states. For the $^2\Pi_u$ state, vibrational analysis was not feasible, so, in this case, a vibrationally averaged asymmetry parameter is reported. The β parameters for the $^2\Sigma_g$, $^2\Sigma_u$ and $^2\Pi_u$ states exhibit features which will aid in analyzing the resonant mechanisms in this spectral range when realistic calculations become available.

The most relevant works related to the present study on cyanogen (ethanedinitrile) are photoabsorption cross-sections [48-50], photoionization cross-sections [51], photoelectron spectroscopy at 21.2 eV [52,53] and 40.8 eV [54], and electron excitation and ionization spectra [55,56]. Theoretical calculations [57-65] have been performed on the molecular orbital sequence, structure, neutral excited state energies, and line strengths. Until recently, a major question has arisen concerning the exact ordering of the four outermost valence orbitals in the molecular ground state. However, this uncertainty now appears to have been resolved, so following the experimental

evidence of Baker and Turner [52] and Turner et al. [53] and more recent calculations [60,61,64], the orbital sequence of cyanogen in its molecular linear ground state may be given as

$$(1\sigma_g)^2(1\sigma_u)^2(2\sigma_g)^2(2\sigma_u)^2(3\sigma_g)^2(3\sigma_u)^2(4\sigma_g)^2(1\pi_u)^4(4\sigma_u)^2(5\sigma_g)^2(1\pi_g)^4$$

The experimental values [52,53] for the four lowest vertical ionization energies are $(1\pi_g)^{-1} {}^2\Pi_g = 13.36$ eV, $(5\sigma_g)^{-1} {}^2\Sigma_g = 14.49$ eV, $(4\sigma_u)^{-1} {}^2\Sigma_u = 14.86$ eV and $(1\pi_u)^{-1} {}^2\Pi_u = 15.47$ eV. The photoionization cross-section [51] of C_2N_2 shows strong resonance structure from close to threshold (13.36 eV) to almost 15.5 eV. This is ascribed [51] to autoionization from at least two Rydberg series which converge onto the ${}^2\Pi_u$ limit. At higher energies, a further, unspecified, Rydberg series is observed, with structure between 18.2 and 19.2 eV. In addition to these peaks which can be identified as being due to autoionization from Rydberg levels, a strong, broad peak is observed extending from approximately 15.5 eV to 20.5 eV, with a maximum at ~ 16.9 eV. One of the purposes of the present investigation was to see whether the photoelectron asymmetry parameters and branching ratios would yield any further information about the nature of this structure.

EXPERIMENTAL

The experiment was performed using a hemispherical electron analyzer [66] coupled to a high aperture (2 m) normal incidence monochromator [67] connected to the Synchrotron Ultraviolet Radiation Facility (SURF II) electron storage ring [68] at the National Bureau of Standards. The monochromator, electron analyzer and experimental method have been described previously and will only be outlined here. The monochromator, incorporating a 1200 lines mm^{-1} osmium-coated grating blazed at about 80 nm, delivered a photon flux of approximately 5×10^{10} photons s^{-1} bandwidth $^{-1}$ at the peak of the output for a spectral resolution of about 0.05 nm (16 meV at 20 eV). The analyzer, based on two copper hemispheres of 50 mm mean radius, with an angular acceptance of $\pm 2^\circ$, was operated in a constant pass energy mode of 5 eV, and could be rotated in a plane at right angles to an incident monochromatic photon beam. The combined resolution of the monochromator and electron analyzer was approximately 110 meV. The polarization of the incoming light was measured by a three-mirror polarization analyzer [69] which rotated with the electron analyzer. As the light from the monochromator was polarized elliptically, the differential cross-section in the dipole approximation, assuming randomly oriented target molecules, and electron angle analysis perpendicular to the photon propagation direction, may be written in the form [70,71]

$$d\sigma/d\Omega = (\sigma_{tot}/4\pi)[1 + (\beta/4)(3P \cos 2\theta + 1)] \quad (1)$$

where β is the photoelectron asymmetry parameter, θ is the photoelectron ejection angle relative to the major polarization axis, and $P = (I_{\parallel} - I_{\perp}) / (I_{\parallel} + I_{\perp})$, the polarization of the incoming radiation. At each photon energy reported here, photoelectron spectra encompassing the vibrational progressions that were energetically accessible at a particular photon energy were recorded at the three angles $\theta = 0^\circ$, 45° and 90° . A sample set of data at a photon energy of 18.62 eV is shown in Fig. 1, where the counts in each spectrum have been normalized so that the maximum count in the $\theta = 0^\circ$ spectrum equals 100. In Fig. 1, the vibrationally resolved $(1\pi_g)^{-1} X^2\Pi_g$ band can be observed, followed by the dominant members of the $(5\sigma_g)^{-1} A^2\Sigma_g$ and the $(4\sigma_u)^{-1} B^2\Sigma_u$ states. The $(1\pi_u)^{-1} C^2\Pi_u$ band is unresolved. At each angle, the spectrum was separated into electronic and vibrational components by means of a nonlinear least squares fit to Gaussian line shapes after correcting for the transmission function of the electron analyzer and a small ($< 4\%$) angular correction factor based on the electron spectrometer calibration [72]. By using eqn. (1), vibrationally averaged and vibrationally resolved asymmetry parameters were determined for the vari-

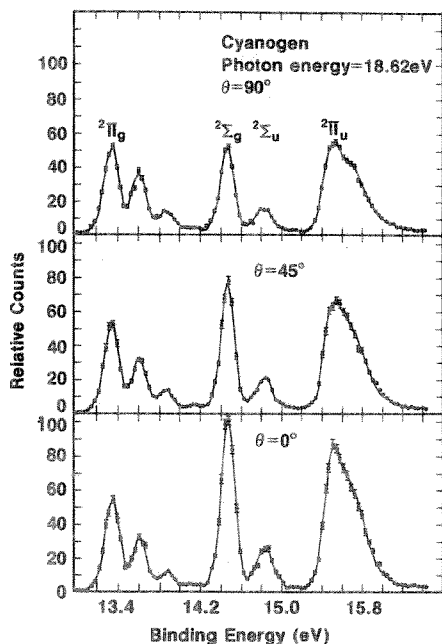


Fig. 1. Photoelectron spectra of cyanogen at a photon energy of 18.62 eV and at $\theta = 0^\circ$, 45° and 90° . The spectra are normalized so that the maximum counts in the $\theta = 0^\circ$ spectrum = 100. The data points (●) and the nonlinear least squares fit curve (—) are indicated [$\lambda(\text{nm}) = 1239.8/E(\text{eV})$].

ous photoelectron bands. Once the asymmetry parameters had been determined, eqn. (1) was again used to calculate the branching ratios of the ionic states and of the vibrational levels within certain bands. The errors associated with the asymmetry parameter data represent a combination of the uncertainty in the nonlinear least squares fit, the degree of agreement between the parameters deduced from the redundant set of measurements at three angles and an estimate of possible systematic errors. The errors in the electronic branching ratios fall within the magnitude of the symbol representing the measurement.

RESULTS

The asymmetry parameters for the four outermost valence orbitals of cyanogen are shown in Fig. 2. For the $(1\pi_g)^{-1} {}^2\Pi_g$ and the $(1\pi_u)^{-1} {}^2\Pi_u$ states the vibrationally averaged values have been plotted, while for the $(5\sigma_g)^{-1} {}^2\Sigma_g$ and the $(4\sigma_u)^{-1} {}^2\Sigma_u$ states the data represent the β parameters of the dominant $v = 0$ member. Figure 3 shows the corresponding electronic state branching ratios. All of the parameters were deduced from least squares fits to the experimental data in which the vibrational structure in the first three bands has been properly accounted for, and the ${}^2\Pi_u$ state, being unresolved, has been analyzed by fitting the area under the band.

With reference to Figs. 2 and 3, several characteristics of the data are noteworthy. First, the ${}^2\Pi_u$ asymmetry parameter increases smoothly with increasing photon energy from a negative value at threshold to approximately 1.0 at 24 eV. This is similar to the behavior of π orbitals in other molecules, e.g., nitrogen and carbon monoxide, and does not suggest any strong resonant behavior in this channel. Second, for the ${}^2\Sigma_u$ state, the β parameter is, on the whole, relatively constant, with localized variations near threshold and near 19 eV, where autoionization structure is known to occur [51]. Third, the ${}^2\Sigma_g$ asymmetry parameter, exhibits a definite, well-defined oscillation between threshold and approximately 19 eV. The steep rise near threshold and subsequent peak around 15.5 eV fall in the midst of observed autoionization structure. However, the dip and subsequent rise, occur in the energy range spanned by a broad feature, with a maximum at ~ 16.9 eV, observed in the photoionization efficiency curve [51]. The origin of this structure in the present results and its relation to the broad feature pose interesting questions. Fourth, the ${}^2\Pi_g$ curve is very similar to the ${}^2\Sigma_g$ curve, although it is shifted to significantly lower values. It shows some additional structure around 17.5 eV and continues to increase up to the high-energy limit of the present measurements. Fifth, the electronic branching ratios in Fig. 3 do not exhibit any major features, other than the relative enhancements in the top three curves near their thresholds. The gradual onset and

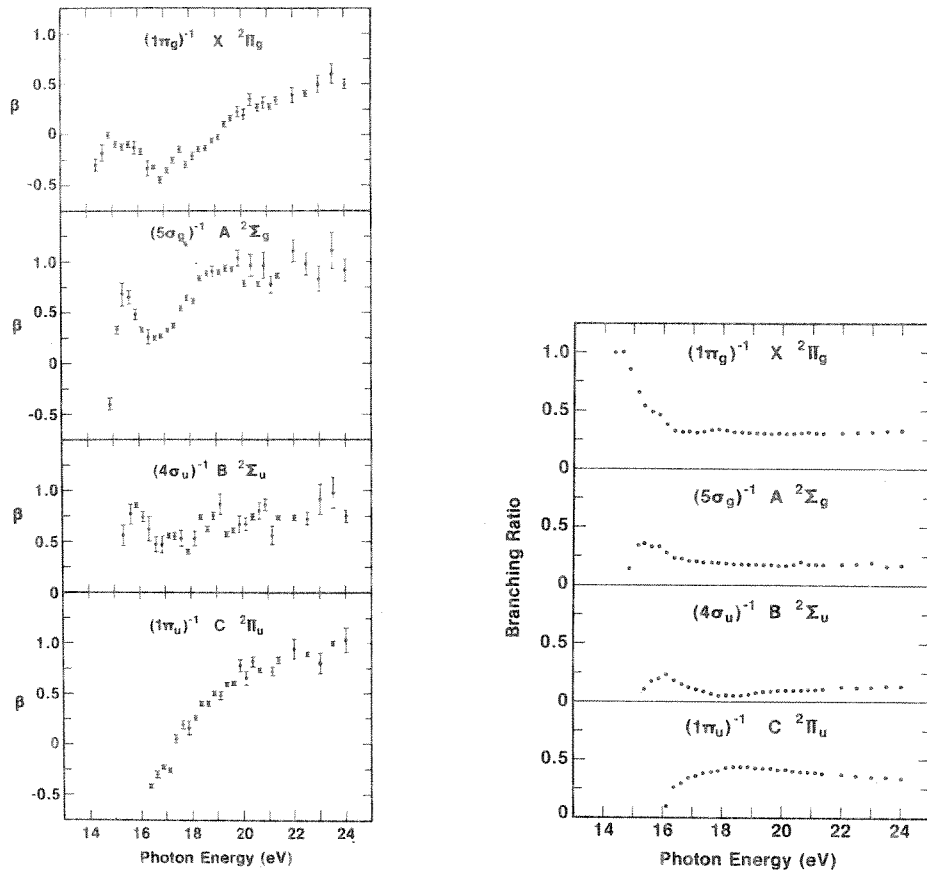


Fig. 2. Photoelectron asymmetry parameters of the four outermost valence orbitals in cyanogen plotted as a function of photon energy [$\lambda(\text{nm}) = 1239.8/E$ (eV)].

Fig. 3. Electronic state branching ratios of the four outermost valence orbitals in cyanogen plotted as a function of photon energy [$\lambda(\text{nm}) = 1239.8/E$ (eV)].

broad hump in the $^2\Pi_u$ curve has no distinct features at all, as in the β parameter for this channel. The weak peak above 17 eV in the $^2\Pi_g$ curve is real and emerges in the vibrational branching ratios for that channel, as discussed below.

The vibrationally resolved results for the $^2\Pi_g$ channel are of direct concern to this discussion, as they are often sensitive to resonant mechanisms. The ground ionic state, $X^2\Pi_g$, photoelectron band shows a progression in ν_1 , the $C\equiv N$ symmetrical stretching mode (where ν_n is the n th normal mode of vibration). The four lowest vibrational members were observed in the present experiment, and the β parameters for $v = 0, 1$ and 2

are shown in Fig. 4. The three curves are similar at first glance but, on closer inspection, exhibit systematic differences which exceed statistical error. In particular, the curves show different local structure up to an energy of approximately 19 eV, above which they exhibit a generally similar shape, although shifted somewhat in magnitude. Therefore, extensive v -dependence is observed, but not in the form of a simple prominent pattern.

The vibrational branching ratios were observed to have fairly constant values of $v = 0$, 52%; $v = 1$, 32%; $v = 2$, 11%; and $v = 3$, 5%; throughout the present photon energy range. However, minor deviations were exhibited, mainly below 18 eV. Therefore, to demonstrate non-Franck-Condon structure, the ratios of the intensities of the $v = 1, 2$ and 3 members to that of the $v = 0$ member have been plotted in Fig. 5. The ratios are generally constant, suggesting Franck-Condon behavior, except below 15.5 eV and between

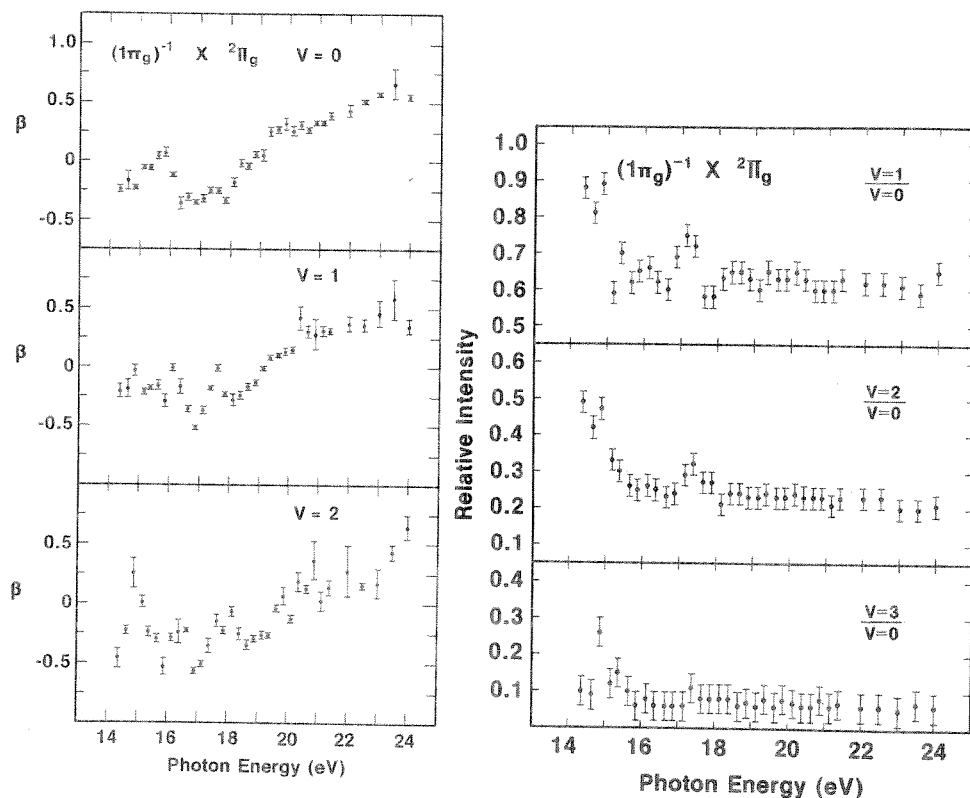


Fig. 4. Vibrationally resolved asymmetry parameters for the $v = 0, 1$ and 2 levels of $C_2N_2^+ X^2\Pi_g$, plotted as a function of photon energy [$\lambda(\text{nm}) = 1239.8/E$ (eV)].

Fig. 5. The ratio of the intensities of the $v = 1, 2$ and 3 members to that of the $v = 0$ member for the $C_2N_2^+ X^2\Pi_g$ state [$\lambda(\text{nm}) = 1239.8/E$ (eV)].

16.5 and 18 eV. These systematic deviations from constant ratios should serve as a clear indicator of resonant effects in future work on cyanogen.

It has been suggested [52,53] that the two outer σ orbitals are the out-of-phase and in-phase combinations of the nitrogen nonbonding orbitals and that photoionization produces very intense $v = 0 \rightarrow 0$ transitions. Baker and Turner [52] and Turner et al. [53] observed a very weak vibrational progression in ν_1 , the symmetric $\text{C}\equiv\text{N}$ stretching mode, with vibrational spacing of 0.231 eV following ionization of a $5\sigma_g$ electron. Our data suggest that the intensity of the $v = 1$ member of the ${}^2\Sigma_g$ band is never greater than 3% of the $v = 0$ member throughout the photon energy range studied in the present experiment. No higher members of the vibrational progression following ionization of the $4\sigma_u$ electron were observed either by Turner et al. [53] or in the present experiment. The vibrational progression for the ${}^2\Pi_u$ state of the ion is complicated. Turner et al. [53] observed progressions in ν_1 and ν_2 and in addition, an indication that the ν_4 frequency mode, the symmetric bending mode, was being excited. The C-C stretch, ν_2 , has an energy of 0.088 eV.

DISCUSSION

To simplify the discussion of the present results, the observed spectral range will be divided into three parts. Region I will extend from the first ionization energy of cyanogen to 15.5 eV. Region II covers the energy range between approximately 15.5 and 18 eV, and Region III begins where Region II ends and includes the high energy portion of the spectrum up to the $4\sigma_g$ threshold at 22.8 eV [61]. Regions I and III contain autoionizing features which have been observed by photoionization mass spectrometry and discussed elsewhere [51]. The autoionization structure in Region I converges onto the A, B and C ionization thresholds and, presumably, that in Region III onto the $(4\sigma_g)^{-1} {}^2\Sigma_g$ threshold. We will not discuss the spectroscopy of the autoionizing states in Regions I and III, but will rely on previous observations of these resonant peaks to account for the sharp variations in the vibrationally resolved parameters in these two regions.

Even such general statements are not presently possible for Region II, as no concrete evidence is available regarding the resonant mechanisms which may have significant effects in this energy range. The photoionization yield curve is certainly suggestive of resonant structure, exhibiting a broad peak centered at approximately 16.9 eV and extending throughout Region II, superimposed upon a non-resonant background. Using what little related information is available, possible contributions to the apparent resonant effects in Region II will be speculated upon. Two main possibilities need to be examined—autoionization and shape resonances.

Regarding shape resonances, Hitchcock and Brion [56] have observed broad continuum features in the pseudo-photon carbon and nitrogen K spectra of both HCN and C_2N_2 , which are believed [73] to be analogous to the σ ($l=3$, where l is the orbital angular momentum) shape resonances in N_2 and CO. These broad features lie approximately 12 eV above their respective ionization energies and correspond to an $l=3$ -type shape resonance localized on the $C\equiv N$ subgroup. Since these trapping sites are off-center in cyanogen, gerade and ungerade linear combinations of the molecular orbitals may be presumably constructed to produce shape resonances in both the σ_u and σ_g ionization continua. However, transitions to these continuum channels from the valence orbitals investigated here would not fall in the spectral range studied, especially considering the tendency for shape resonances to shift approximately 1–3 eV higher in kinetic energy upon going from core spectra to valence shell spectra. Therefore, barring a large and unlikely splitting between the resonance positions in cyanogen, the $C\equiv N$ counterpart to the $l=3$ -like σ resonance in N_2 and CO does not seem to play a role in C_2N_2 photoionization dynamics until higher photon energies are used.

It is interesting to consider another conceivable shape resonance mechanism, that is, trapping on the C–C site. This is highly speculative, but there is some evidence supporting the possibility:

(a) Fridh et al. [61] calculate the location of a $5\sigma_u$ valence orbital at 4.93 eV in the continuum (in quantum chemistry terms). This would correspond to a σ_u shape resonance in scattering language and could be the C–C site analogue of the σ_u shape resonance in nitrogen. This 5σ orbital of cyanogen has large contributions on the carbon centers. Fridh et al. allow for some uncertainty in its location since lack of empirical evidence made it difficult to parameterize this state in the hydrogen atoms in molecules by their procedure (HAM/3). Accordingly, in the $1\pi_g$ ionization channel, the $5\sigma_u$ resonant state would lie at a photon energy of approximately 18 eV, with a 2–3 eV uncertainty. Note that the corresponding broad feature at 17 eV in the electron excitation spectrum of cyanogen was tentatively interpreted as $5\sigma_g \rightarrow 5\sigma_u$. The predicted transition energy of 20.0 eV led to an even greater energy discrepancy than for the assignment being considered.

(b) An unrelated multiple-scattering model calculation [74] on the K-shell spectrum of C_2 , using an internuclear separation of 1.5 Å, produced a σ_u f-type resonance at 2.8 eV kinetic energy. However, the C–C distance in C_2N_2 is 1.380 Å. Generally, shape resonances move to higher energy as the internuclear separation decreases, assuming relatively small changes. Hence, the kinetic energy at which the C–C shape resonance occurs in cyanogen could be expected to be greater than 2.8 eV. However, the uncertainty is a few eV. This fragment of evidence would provide some support for a

low-lying resonance in the $1\pi_g$ channel in Region II.

(c) The carbon K-shell spectrum exhibits a strong non-Rydberg peak very near threshold. A weaker one also occurs in the nitrogen K-shell spectrum just above threshold. In converting a K-shell shape resonance position to a valence shell position, it is usually necessary to add 1–3 eV on the kinetic energy scale. This would place the indicated features from the K-shell spectra a few eV above the $1\pi_g$ ionization energy in the valence shell spectra. We emphasize that there is no solid evidence for this conjecture but it is important that even tentative shape resonance assignments should not be inconsistent with inner shell spectra.

(d) Finally, by similar reasoning to that given in (b), the lower kinetic energy of the σ_u resonance on the C–C site relative to the $C\equiv N$ site could be qualitatively rationalized on the basis of the much larger internuclear distance (1.380 Å and 1.157 Å, respectively).

To summarize, there is some evidence suggesting the possibility of a $5\sigma_u$ shape resonance (or valence state in its own continuum) in Region II.

The other mechanism to be explored is the possible presence of an autoionizing valence state converging onto a higher ionization threshold. This proved to be the case for similar broad features in acetylene [75,76]. Again, the calculation of Fridh et al. [61] contains a possibility. They estimate the location of the $4\sigma_g \rightarrow 2\pi_u$ intravalence transition in cyanogen to be at approximately 15 eV. Considering the possibility of additional interaction between the $2\pi_u$ state (itself a shape resonantly-enhanced bound state related to the $1\pi_g$ state in N_2) and the $4\sigma_g$ hole, the uncertainty in this transition energy does not rule out its occurrence in Region II.

To summarize, we have found some evidence for a resonant process in Region II which could be either a $5\sigma_u$ shape resonance or an intravalence $4\sigma_g \rightarrow 2\pi_u$ autoionizing transition, or possibly contributions from both. It would be interesting to consider these possibilities, along with others not identified, in a theoretical treatment of the non-Franck–Condon and other dynamical effects in Region II. The best experimental evidence would appear to be the peak at ~ 17 – 17.5 eV in the ratios of vibrational intensities (Fig. 5), and the shape of the β curves (Figs. 2 and 4) in Region II. If the shape resonance mechanism is active, a realistic, independent-electron calculation should produce the essential aspects of the observed effects, and some manifestations should be observed in all the gerade initial states. If autoionization is the underlying mechanism, a multichannel treatment would be required to yield the dynamical effects reported here. In any case, it is hoped that these new data and this speculative discussion will stimulate theoretical studies needed to clarify the questions raised in this paper.

ACKNOWLEDGMENTS

We wish to thank R.P. Madden for his support and encouragement throughout this work. We appreciate the valuable assistance provided by G. Rakowsky and the staff of the National Bureau of Standards' SURF II facility. This work was supported in part by the Office of Naval Research, the U.S. Department of Energy and NATO Grant No. 1939.

REFERENCES

- 1 J.L. Dehmer, D. Dill and A.C. Parr, in S. McGlynn, G. Findley and R. Huebner (Eds.), *Photophysics and Photochemistry in the Vacuum Ultraviolet*, D. Reidel, Dordrecht, Holland, 1983, in press.
- 2 V. Schmidt, *Appl. Opt.*, 19 (1980) 4080; R.P. Madden and A.C. Parr, *Appl. Opt.*, 21 (1982) 179.
- 3 G. Herzberg, *Molecular Spectra and Molecular Structure III, Electronic Spectra and Electronic Structure of Polyatomic Molecules*, Van Nostrand Reinhold Company, New York, 1966.
- 4 E.W. Plummer, T. Gustafsson, W. Gudat and D.E. Eastman, *Phys. Rev. A.*, 15 (1977) 2339.
- 5 G.V. Marr, J.M. Morton, R.M. Holmes and D.G. McCoy, *J. Phys. B.*, 12 (1979) 43.
- 6 J.B. West, A.C. Parr, B.E. Cole, D.L. Ederer, R. Stockbauer and J.L. Dehmer, *J. Phys. B.*, 13 (1980) L105.
- 7 T.A. Carlson, M.O. Krause, D. Mehaffy, J.W. Taylor, F.A. Grimm and J.D. Allen, *J. Chem. Phys.*, 73 (1980) 6056.
- 8 S. Krummacher, V. Schmidt and F. Wuilleumier, *J. Phys. B.*, 13 (1980) 3993.
- 9 R. Stockbauer, B.E. Cole, D.L. Ederer, J.B. West, A.C. Parr and J.L. Dehmer, *Phys. Rev. Lett.*, 43 (1979) 757.
- 10 B.E. Cole, D.L. Ederer, R. Stockbauer, K. Codling, A.C. Parr, J.B. West, E.D. Poliakoff and J.L. Dehmer, *J. Chem. Phys.*, 72 (1980) 6308.
- 11 D.G. McCoy, J.M. Morton and G.V. Marr, *J. Phys. B.*, 11 (1978) L547.
- 12 T. Gustafsson, *Chem. Phys. Lett.*, 75 (1980) 505.
- 13 P. Morin, I. Nenner, P.M. Guyon, O. Dutuit and K. Ito, *J. Chim. Phys.*, 77 (1980) 605.
- 14 A. Tabche-Fouhaile, I. Nenner, P.M. Guyon and J. Delwiche, *J. Chem. Phys.*, 75 (1981) 1129.
- 15 S. Southworth, C.M. Truesdale, P.H. Kobrin, D.W. Lindle, W.D. Brewer and D.A. Shirley, *J. Chem. Phys.*, 76 (1982) 143.
- 16 T.A. Carlson, M.O. Krause, F.A. Grimm, J.D. Allen, D. Mehaffy, P.R. Keller and J.W. Taylor, *Phys. Rev. A.*, 23 (1981) 3316.
- 17 T.A. Carlson, M.O. Krause, F.A. Grimm, J.D. Allen, D. Mehaffy, P.R. Keller and J.W. Taylor, *J. Chem. Phys.*, 75 (1981) 3288.
- 18 T.A. Carlson, M.O. Krause and F.A. Grimm, *J. Chem. Phys.*, 77 (1982) 1701.
- 19 R. Unwin, I. Khan, N.V. Richardson, A.M. Bradshaw, L.S. Cederbaum and W. Domcke, *Chem. Phys. Lett.*, 77 (1981) 242.
- 20 P.W. Langhoff, B.V. McKoy, R. Unwin and A.M. Bradshaw, *Chem. Phys. Lett.*, 83 (1981) 270.
- 21 A.C. Parr, D.L. Ederer, J.B. West, D.M.P. Holland and J.L. Dehmer, *J. Chem. Phys.*, 76 (1982) 4349.

- 22 P.R. Keller, D. Mehaffy, J.W. Taylor, F.A. Grimm and T.A. Carlson, *J. Electron Spectrosc. Relat. Phenom.*, 27 (1982) 223.
- 23 D.M.P. Holland, J.B. West, A.C. Parr, D.L. Ederer, R. Stockbauer, R.D. Buff and J.L. Dehmer, *J. Chem. Phys.*, 78 (1983) 124.
- 24 D. Mehaffy, P.R. Keller, J.W. Taylor, T.A. Carlson, M.O. Krause, F.A. Grimm and J.D. Allen, *J. Electron Spectrosc. Relat. Phenom.*, 26 (1982) 213.
- 25 J.W. Davenport, *Phys. Rev. Lett.*, 36 (1976) 945.
- 26 T.N. Rescigno, C.F. Bender, B.V. McKoy and P.W. Langhoff, *J. Chem. Phys.*, 68 (1978) 970.
- 27 S. Wallace, D. Dill and J.L. Dehmer, *J. Phys. B.*, 12 (1979) L417.
- 28 J.L. Dehmer, D. Dill and S. Wallace, *Phys. Rev. Lett.*, 43 (1979) 1005.
- 29 F.A. Grimm, T.A. Carlson, W.B. Dress, P. Agron, J.O. Thomson and J.W. Davenport, *J. Chem. Phys.*, 72 (1980) 3041.
- 30 R.R. Lucchese and V. McKoy, *J. Phys. B.*, 14 (1981) L629.
- 31 P.W. Langhoff, S.R. Langhoff, T.N. Rescigno, J. Schirmer, L.S. Cederbaum, W. Domcke and W. Von Niessen, *Chem. Phys.*, 58 (1981) 71.
- 32 R.R. Lucchese, G. Raseev and V. McKoy, *Phys. Rev. A.*, 25 (1982) 2572.
- 33 N. Padial, G. Csanak, B.V. McKoy and P.W. Langhoff, *J. Chem. Phys.*, 69 (1978) 2992.
- 34 B. Ritchie and B.R. Tambe, *J. Phys. B.*, 13 (1980) L225.
- 35 J.A. Stephens, D. Dill and J.L. Dehmer, *J. Phys. B.*, 14 (1981) 3911.
- 36 A. Gerwer, C. Asaro, B.V. McKoy and P.W. Langhoff, *J. Chem. Phys.*, 72 (1980) 713.
- 37 G. Raseev, H. Lefebvre-Brion, H. LeRouzo and A.L. Roche, *J. Chem. Phys.*, 74 (1981) 6686.
- 38 P.M. Dittman, D. Dill and J.L. Dehmer, *J. Chem. Phys.*, 76 (1982) 5703.
- 39 S. Wallace, D. Dill and J.L. Dehmer, *J. Chem. Phys.*, 76 (1982) 1217.
- 40 J.R. Swanson, D. Dill and J.L. Dehmer, *J. Phys. B.*, 13 (1980) L231.
- 41 J.R. Swanson, D. Dill and J.L. Dehmer, *J. Phys. B.*, 14 (1981) L207.
- 42 N. Padial, G. Csanak, B.V. McKoy and P.W. Langhoff, *Phys. Rev. A.*, 23 (1981) 218.
- 43 R.R. Lucchese and V. McKoy, *J. Phys. Chem.*, 85 (1981) 2166.
- 44 L.E. Machado, E.P. Leal, G. Csanak, B.V. McKoy and P.W. Langhoff, *J. Electron Spectrosc. Relat. Phenom.*, 25 (1982) 1.
- 45 J.L. Dehmer and D. Dill, in T. Rescigno, V. McKoy and B. Schneider (Eds.), *Electron-Molecule and Photon-Molecule Collisions*, Plenum Press, New York, 1979, pp. 225-265.
- 46 D.M.P. Holland, A.C. Parr and J.L. Dehmer, *J. Phys. B.*, to be submitted.
- 47 D.M.P. Holland, A.C. Parr and J.L. Dehmer, to be published.
- 48 S. Woo and T. Liu, *J. Chem. Phys.*, 5 (1937) 161.
- 49 W.C. Price and A.D. Walsh, *Trans. Faraday Soc.*, 41 (1945) 381.
- 50 R.E. Connors, J.L. Roebber and K. Weiss, *J. Chem. Phys.*, 60 (1974) 5011.
- 51 V.H. Dibeler and S.K. Liston, *J. Chem. Phys.*, 47 (1967) 4548.
- 52 C. Baker and D.W. Turner, *Proc. R. Soc. London, Ser. A.*, 308 (1968) 19.
- 53 D.W. Turner, C. Baker, A.D. Baker and C.R. Brundle, *Molecular Photoelectron Spectroscopy*, Wiley-Interscience, London, 1970, pp. 345-355.
- 54 L. Asbrink, W. Von Niessen and G. Bieri, *J. Electron Spectrosc. Relat. Phenom.*, 21 (1980) 93.
- 55 C.A. McDowell and J.W. Warren, *Trans. Faraday Soc.*, 48 (1952) 1084.
- 56 A.P. Hitchcock and C.E. Brion, *Chem. Phys.*, 37 (1979) 319.
- 57 E. Clementi and A.D. McLean, *J. Chem. Phys.*, 36 (1962) 563.
- 58 E. Clementi and H. Clementi, *J. Chem. Phys.*, 36 (1962) 2824.

- 59 J.M. Hollas and T.A. Sutherley, *Mol. Phys.*, 24 (1972) 1123.
- 60 L.S. Cederbaum, W. Domcke and W. Von Niessen, *Chem. Phys.*, 10 (1975) 459.
- 61 C. Fridh, L. Åsbrink and E. Lindholm, *Chem. Phys.*, 27 (1978) 169.
- 62 S. Bell, *Chem. Phys. Lett.*, 67 (1979) 498.
- 63 G. Bieri, E. Heilbronner, V. Hornung, E. Kloster-Jenson, J.P. Maier, F. Thommen and W. Von Niessen, *Chem. Phys.*, 36 (1979) 1.
- 64 L.S. Cederbaum, W. Domcke, J. Schirmer and H. Koeppel, *J. Chem. Phys.*, 72 (1980) 1348.
- 65 N.N. Haese and R.C. Woods, *J. Chem. Phys.*, 73 (1980) 4521.
- 66 A.C. Parr, R. Stockbauer, B.E. Cole, D.L. Ederer, J.L. Dehmer and J.B. West, *Nucl. Instrum. Methods*, 172 (1980) 357.
- 67 D.L. Ederer, B.E. Cole and J.B. West, *Nucl. Instrum. Methods*, 172 (1980) 185.
- 68 R.P. Madden, *Nucl. Instrum. Methods*, 172 (1980) 1.
- 69 V.G. Horton, E.T. Arakawa, R.N. Hamm and M.W. Williams, *Appl. Opt.*, 8 (1969) 667.
- 70 J.A.R. Samson and J.L. Gardner, *J. Opt. Soc. Am.*, 62 (1972) 856.
- 71 J.A.R. Samsom and A.F. Starace, *J. Phys. B.*, 8 (1975) 1806.
- 72 D.M.P. Holland, A.C. Parr, D.L. Ederer, J.L. Dehmer and J.B. West, *Nucl. Instrum. Methods*, 195 (1982) 331.
- 73 J.L. Dehmer, J. Siegel and D. Dill, Argonne National Laboratory Radiological and Environmental Research Division Annual Report, 1978, pp. 59-61.
- 74 P.M. Dittman, private communication, 1982.
- 75 A.C. Parr, D.L. Ederer, J.L. Dehmer and D.M.P. Holland, *J. Chem. Phys.*, 77 (1982) 111.
- 76 T. Hayaishi, S. Iwata, M. Sasunuma, E. Ishiguro, Y. Morioka, Y. Iida and M. Nakamura, *J. Phys. B.*, 15 (1982) 179.